High-pressure studies of topological materials

Sergey Medvedev[#], Qingge Mu, Yanpeng Qi, Pavel Naumov, Moaz ElGhazali, Claudia Felser

Exotic quantum-mechanical properties and potential applications of materials with topologically nontrivial electronic structures have recently attracted much attention. The application of an external pressure to drive topological quantum-phase transitions is an effective method for obtaining a better understanding of topologically nontrivial phases by elucidating the interaction between different ground states. Achieving a superconducting state in topological materials is of particular interest as an important step toward topological superconductors. Here, we map the electronic and structural phase diagrams of topologically nontrivial materials by evaluating the electronic transport properties (electrical resistivity, Hall effect, and magnetoresistance), and chemical structure (by Raman spectroscopy and synchrotron x-ray diffraction) at high pressures. To gain insight into pressure-driven electronic transitions, experimental studies are accompanied by theoretical calculations of the electronic band structure.

Topologically nontrivial materials are a class of materials with novel quantum-mechanical properties. They have recently gained much attention because of their exotic electronic properties that enable potential applications in electronics, spintronics, opto-electronics, and quantum computation. These materials host new quantum states of matter that are characterized by unique edge or surface states that appear due to the topological character of the bulk wave functions. The special electronic structure of topological materials gives rise to interesting electronic properties, such as chiral magnetic effects, negative magnetoresistance, and the quantum anomalous Hall effect. Of special interest is achieving a super-conducting state in topological materials since the realization of superconductivity in topological compounds is regarded as an important step toward topological superconductors.

To better understand new topologically nontrivial phases of matter, it is useful to investigate the competition between different topologically trivial and nontrivial ground states and emerging phenomena by tuning the system with different external parameters, such as temperature, magnetic field, pressure, and chemical doping. Although high-pressure phases of matter have limited direct applications, performing experiments under pressure is an invaluable tool for evaluating new phases of matter because the crystal structure can be easily modified without the addition of impurities and defects. Such variations in the crystal structure usually result in changes in the electronic structures and topological states. Electrical transport experiments play a key role in the study of the electronic properties of matter under extreme conditions, including interesting phenomena such as insulator-to-metal transitions, quantum critical phenomena, pressure-induced superconductivity, and electronic topological transitions.

Pressure-induced electronic topological transitions

Systematic pressure-dependent studies of the family of Weyl semimetals (e.g., NbP, NbAs, and TaAs) revealed a common anomaly in the pressure dependence of their electrical resistivity. [1, 2] The resistivity initially decreases with increasing pressure, and then increases as the pressure increases above a critical value p_c ~9 GPa, ~11 GPa, and ~16 GPa for NbP, NbAs, and TaAs, respectively (Fig. 1). Experimental structural and Raman spectroscopy analyses, accompanied by theoretical density functional theory calculations of the electronic structure of this family of materials showed that these anomalies are associated with a pressure-induced Lifshitz transition, which involves the appearance of electron and hole pockets in the electronic structure of these materials. [1, 2]

The anomalous behavior of the resistivity as a signature of an electronic topological transition is also observed for the quasi-one-dimensional topological material β-Bi_4I_4 hosting highly anisotropic surface-

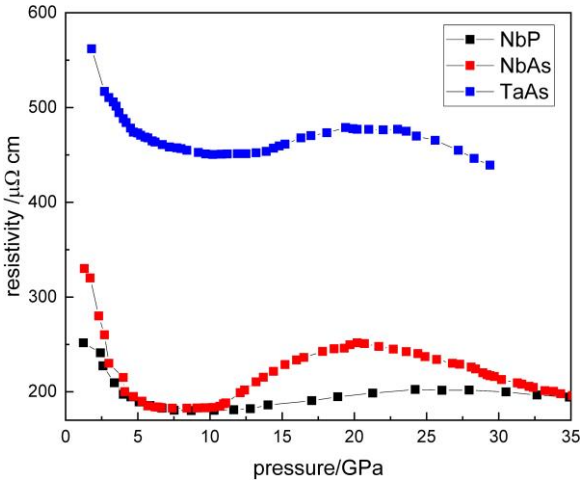

Fig. 1: Pressure dependence of the electrical resistivity of NbP, NbAs, and TaAs at room temperature.

state Dirac fermions. [3] The resistivity of β-Bi_4I_4 exhibits a non-monotonic evolution with increasing pressure (Fig. 2a). At low pressures, the resistivity is first suppressed with applied pressure and reaches a minimum value at ~3 GPa. Upon further increasing the pressure, the resistivity gradually increases, reaching a maximum at a pressure above 8 GPa. As the pressure is further increased above 8.8 GPa, the resistivity rapidly decreases, while the temperature dependence of the resistivity exhibits semiconductor-like behavior. [3] As the pressure increases up to 13.5 GPa, the temperature dependence of the resistivity shows metallic behavior indicating an insulator-to-metal transition. [3] Furthermore, superconductivity is observed in the metallic phase of Bi_4I_4. The superconducting transition temperature T_c increases with applied pressure, and a typical dome-like evolution is obtained at a maximum T_c of 6 K under a pressure of 23 GPa (Fig. 2a).

These results demonstrated that the application of high pressure dramatically alters the electronic properties of β-Bi_4I_4. A comprehensive understanding of the physical properties of β-Bi_4I_4 is further provided by density functional theory calculations of the electronic band structures. From the band structure at zero pressure, β-Bi_4I_4 is in a strong topological insulator

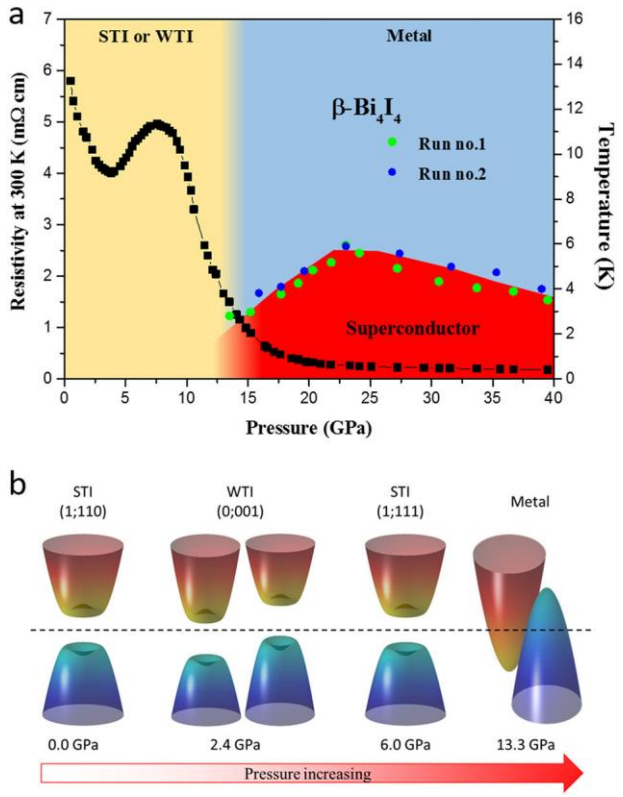

Fig. 2: (a) Electronic pressure–temperature phase diagram of β-Bi_4I_4. (b) Schematic illustration of the band structure evolution under pressure.

(STI) phase with a band inversion at the Y point of the Brillouin zone. As pressure increases, the conduction band minimum and the valence band maximum meet at the M point of the Brillouin zone. Band inversion occurs and the electronic structure is driven into a weak topological insulator (WTI) phase. During band inversion, the band gap decreases to zero and then reopens. Therefore, the resistivity decreases before the band gap closes and then increases after the band gap reopens. This trend is generally consistent with the experimental resistivity values (see Fig. 2). When pressure continues increasing, the band at the Y point is inverted back, and the electronic structure returns to the STI phase. [3] This band evolution is schematically presented in Fig. 2b. Finally, further pressure increase leads to band overlap and pressure-induced metallization. The results demonstrate unusual multiple topological quantum phase transitions in Bi_4I_4. [3]

Experimental technique development

To better understand the electronic structure of crystals, it is crucial to evaluate the fundamental electrical transport variables, such as the carrier density and mobility as a function of the thermodynamic parameters (temperature, pressure, magnetic field). In addition, measurements of the magnetotransport properties (magnetoresistance and Hall-effect) are crucial for inferring information about the interactions between itinerant charge carriers and the magnetic degrees of freedom in a variety of magnetic materials. [4] However, performing *in situ* Hall-effect measurements in diamond anvil cells under high pressure is still challenging. To perform electronic magnetotransport measurements, we developed a measurement setup utilizing the van der Pauw technique in a diamond anvil cell. This technique is widely and successfully used to measure the pressure dependence of the electrical resistivity ρ_{xx}, in combination with other experimental techniques (e.g., synchrotron Mössbauer spectroscopy in an applied magnetic field [5]). However, a major problem when performing Hall-effect measurements at high pressure is the large offset voltage caused by asymmetric contact placement and irregular sample shapes. The most convenient way to overcome this problem is to perform Hall measurements with magnetic-field sweeping, where two sets of Hall measurements are obtained (one in the positive and one in the negative magnetic-field direction. The measurements could be performed using a commercial Physical Properties Measurements System (Quantum Design PPMS) or a

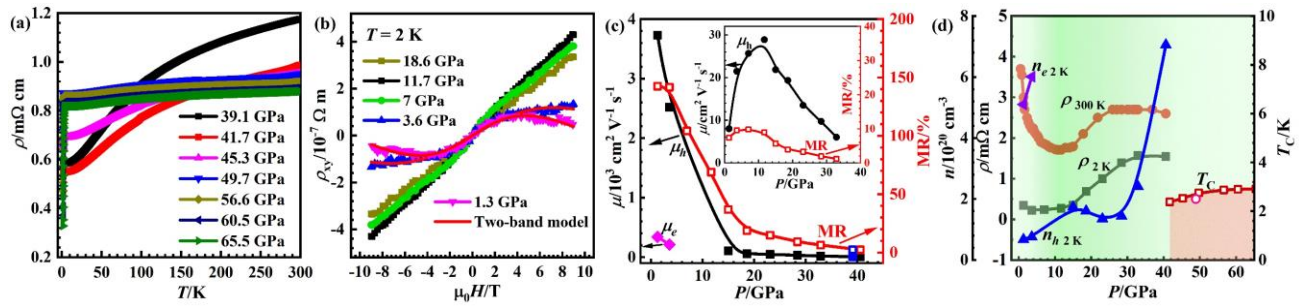

Fig. 3: Effect of pressure on the electronic transport properties of $NbIrTe_4$. (a) Temperature dependence of the resistivity at high pressure. (b) Hall resistivity as a function of different pressures. (c) Pressure dependence of the carrier mobilities and magnetoresistance. (d) High-pressure phase diagram of $NbIrTe_4$.

custom measurement setup using an Oxford Instruments 9T cryomagnet. This technique enables the measurement of electrical properties, such as the Hall voltage (V_H), Hall coefficient (R_H), conductivity type, carrier mobility (μ) and concentration (n), electrical resistivity (ρ), magnetoresistance (R_B), and current–voltage (I-V) characteristics. All of these properties can be measured as a function of pressure (up to 100 GPa), temperature (1.5–300 K), and magnetic field (up to 9 T). This technique was used to study the effect of pressure on the electronic properties of the Weyl semimetals $NbIrTe_4$ and $(TaSe_4)_2I$.

Pressure-dependent changes of the Fermi surface and superconductivity in $NbIrTe_4$

The ternary compounds *MM*'Te_4 (*M* = Nb, Ta, *M*' = Ir, Rh) were proposed theoretically and experimentally confirmed to be type-II Weyl semimetals. $NbIrTe_4$ has an orthorhombic lattice structure without inversion symmetry, which can be considered as a ternary variant of WTe_2. Angle-resolved photoemission spectroscopy studies showed two different Fermi arc connections on opposite terminations of (001) crystal faces. High magnetoresistance values were measured, and no saturation was observed up to a field of 35 T. Quantum oscillation studies revealed that the Fermi surface of $NbIrTe_4$ is very sensitive to changes in the chemical potential, while the Weyl points persist against the shift of the Fermi level, as predicted by theoretical calculations. These features make $NbIrTe_4$ a good platform to study the effect of pressure on its topological properties.

The pressure-dependent electronic transport properties of $NbIrTe_4$ were systematically studied up to ~65 GPa (Fig. 3). [6] The sample showed metallic behavior up to the highest measured pressure, similar to the ambient-pressure data (Fig. 3a). Interestingly, the pressure dependence of the electrical resistivity is not monotonic. As shown in Fig. 3d, the resistivity at room temperature (300 K) decreased to a minimum as the pressure approaches ~ 12 GPa and then increased as the pressure is further increased. This behavior is similar to that in the systems described above that undergo pressure-induced electronic topological transitions. To study the pressure-dependent electronic structure, measurements of the Hall resistivity $\rho_{xy}(B)$ and magnetoresistance MR(B) [6] were performed at high pressures. At 1.3 GPa, the sign of the slope for $\rho_{xy}(B)$ changes from positive to negative as the magnetic field increases from 0 T to 9 T (Fig. 3b), similar to the behavior at ambient pressure [6]. This suggests that the multiband character of the Fermi surface at ambient pressure persists at elevated pressures, where the major carriers are electrons with low mobility. The multiband feature survives up to 11.7 GPa, as indicated by the nonlinear $\rho_{xy}(B)$ curves (Fig. 3b). However, with further increase in pressure, the $\rho_{xy}(B)$ curves show a linear magnetic-field dependence (Fig. 3b), indicating that holes are the main charge carriers in this region. This experimental observation is consistent with the results of theoretical calculations demonstrating that holes dominate the Fermi surface at high lattice compression of $NbIrTe_4$. [6] The slope of the linear $\rho_{xy}(B)$ curves becomes larger when the pressure approaches 23.1 GPa, and is followed by a reduction upon further compression, implying that the concentration of holes first decreases slightly and then increases. The carrier densities and mobilities deduced from the analysis of magnetotransport data within the two-band model are shown in Fig. 3c, d.

Finally, when the pressure was increased above 39 GPa, a decrease in the resistivity was observed below 2 K (Fig. 3a), indicating the onset of a superconducting transition. Superconductivity is observed in the pressure range where the concentration of the hole carriers is strongly enhanced (Fig. 3d). The T_c increases with increasing pressure (Fig 3d), while Raman

spectroscopy studies indicate preservation of the ambient-pressure structure of $NbIrTe_4$ over the entire studied pressure range. The observation of superconductivity in $NbIrTe_4$ is similar to the results recently published on isostructural $TaIrTe_4$. Thus, these findings suggest that superconductivity under compression is an intrinsic property of this class of compounds. The modification of the Fermi surface and the increase in the carrier density play a significant role in the pressure-induced superconductivity. Furthermore, the results of electronic band calculations demonstrated the persistence of the Weyl points near the Fermi level up to highly reduced unit-cell volumes (-17%), indicating that $NbIrTe_4$ is a candidate topological superconductor.

Suppression of axionic charge density wave in Ta_2Se_8I

In their parent state, Weyl semimetals are materials in which low-energy electronic quasiparticles behave as chiral relativistic fermions without a rest mass, known as Weyl fermions. Weyl fermions exist at isolated crossing points of the conduction and valence bands (Weyl nodes) and their energy can be approximated with a linear dispersion relation. By activating strong electron–phonon interactions, a charge density wave (CDW) can emerge. A CDW is an ordered quantum fluid of electrons that forms a standing-wave pattern along the atomic chains, which links two Weyl nodes of different chirality and opens gaps at the Weyl crossing points. Recently, signatures of such an axionic CDW were found in the quasi-one-dimensional Weyl semimetal Ta_2Se_8I, resulting in the observation of a dynamic condensed-matter axion quasiparticle. The Ta atoms in the body-centered tetragonal lattice are surrounded by Se_4 rectangles and form chains aligned along the *c* axis. These chains are separated by I ions. Upon cooling below the CDW threshold temperature T_{CDW}= 263 K, Ta_2Se_8I undergoes a CDW transition at ambient pressure. The wave vector of the CDW is incommensurate with the lattice, and the phason is generally pinned to impurities. Therefore, only upon applying a certain threshold electric field (above which the electric force exceeds the pinning forces), the phason is de-pinned and free to slide over the lattice, thereby contributing to the electrical conduction. The resulting conduction behavior is strongly nonlinear and is a characteristic feature of the CDW state. To date, Ta_2Se_8I is the only material in which a combination of the CDW and chiral anomaly has been demonstrated. To map the region where this axionic CDW exists, we combined magnetotransport measurements, Raman

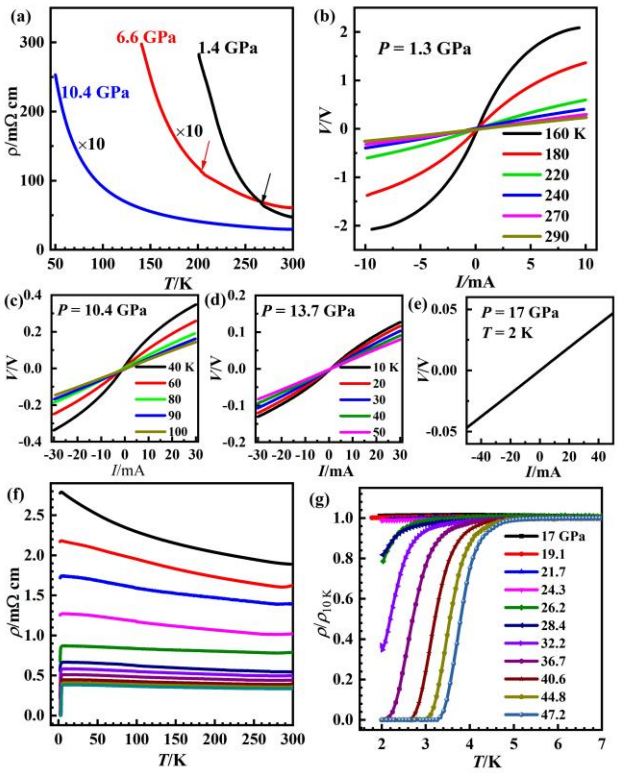

Fig. 4: Effect of pressure on the electronic transport properties of Ta_2Se_8I. (a) Temperature dependence of the resistivity at elevated pressure. The arrows indicate a kink due to CDW-formation (b-e) V-I characteristics at different pressures. (f) Electrical resistivity of Ta_2Se_8I at high pressures. (d) Superconductivity of Ta_2Se_8I at high pressure.

spectroscopy, and *ab initio* calculations to assess its phase diagram. [7]

Figure 4(a) shows the electrical resistivity of Ta_2Se_8I as a function of temperature at various pressures. At low pressures, a faint kink in the resistivity curves (Fig. 4a) indicates the formation of the CDW at T_{CDW}. Consistent with a sliding phason mode, the *V-I* curves were nonlinear below T_{CDW} at high bias currents (Fig 4b). For pressures above 10 GPa, the signature of the CDW transition in the resistivity curves was unclear (Fig. 4a), but the crossover from a linear *V-I* curve at high temperatures to a nonlinear *V-I* curve at low temperatures remained observable (Fig. 4c, d). Finally, the *V-I* curve became linear at the lowest studied temperature (2 K) as the pressure was increased to 17 GPa (Fig. 4e), indicating complete suppression of CDW formation. Hall measurements above T_{CDW} showed that the carrier concentration increases with increasing pressure, [7] indicating an increase in the Fermi surface area at higher pressure. This suggests that the Weyl points move away from the Fermi level with increasing pressure.

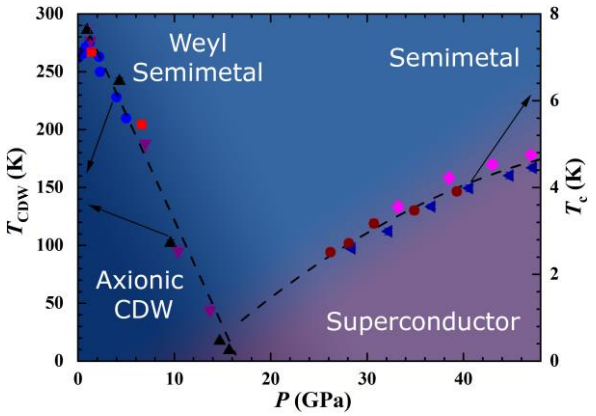

Fig. 5: Phase diagram of Ta_2Se_8I showing the pressure dependence of the CDW transition and superconductivity at pressures up to 47 GPa.

Remarkably, above 20 GPa (the pressure where the CDW is suppressed), a decrease in the resistivity was observed at low temperatures (Fig. 4f, g), indicating the onset of a superconducting transition. The superconducting state is clearly observed at higher pressures, where the resistivity dropped abruptly to zero when reaching T_c (Fig. 4g). With increasing pressure, T_c increases monotonically and was 4.5 K at the maximum measured pressure (47.2 GPa). The state above T_c remains semi-metallic (Fig. 4f).

To gain a deeper understanding of the different states in the pressure phase diagram of Ta_2Se_8I, pressure-dependent Raman spectroscopy and synchrotron x-ray diffraction (XRD) studies were performed. Both sets of data indicated the stability of the ambient-pressure phase of Ta_2Se_8I up to ~20 GPa. Upon further pressure increase, pressure-induced amorphization was indicated by the disappearance of some XRD peaks and the majority of the Raman peaks. [7] In addition, the strongest Raman peak (corresponding to the intrachain Se–Se stretching vibrations) was observed up to the highest experimental pressures, indicating the preservation of the $TaSe_4$ units as building blocks of local order in the high-pressure amorphous phase of Ta_2Se_8I. [7] Based on the electronic band structure calculations, amorphization occurs at pressures where I *p*-bands hybridize at the Fermi level. [7]

A complete phase diagram of Ta_2Se_8I summarizing the newly discovered physics which emerges from the experimental results and theoretical calculations is shown in Fig. 5. At ambient pressure, Ta_2Se_8I is a Weyl semimetal that exhibits a phase transition to an axionic CDW state below T_{CDW}= 263 K. With increasing pressure, the transition temperature and consequently, the gap size, is successively reduced. At 18.2 GPa, the CDW state is fully suppressed, the quasi-one-dimensional behavior vanishes, and a partial amorphization accompanied by a superconducting transition emerges. The T_c continuously increases up to 4.5 K at the highest applied pressure (47.2 GPa).

References

[1] *Pressure-induced Lifshitz transition in NbP: Raman, x-ray diffraction, electrical transport, and density functional theory, S. N. Gupta, A. Singh, K. Pal, D. V. S. Muthu, C. Shekhar, Y. Qi, P. G. Naumov, S. A. Medvedev, C. Felser, U. V. Waghmare, and A. K. Sood, Phys. Rev. B **97** (2018) 064102.*

[2] *Pressure-induced Lifshitz and structural transitions in NbAs and TaAs: experiments and theory, S. N. Gupta, A. Singh, K. Pal, D. V. S. Muthu, C. Shekhar, M. Elghazali, P.G. Naumov, S. A. Medvedev, C. Felser, U. V. Waghmare, and A. K. Sood, J. Phys.: Condens. Matter **30** (2018) 185401.*

[3] *Pressure-induced superconductivity and topological quantum phase transitions in a quasi-one-dimensional topological insulator: Bi_4I_4, Y. Qi, W. Shi, P. Werner, P. G. Naumov, W. Schnelle, L. Wang, K. Rana, S. Parkin, S. A. Medvedev, B. Yan, and C Felser, npj Quantum Materials **3** (2018) 4.*

[4]* *$Mn_{1/4}NbS_2$: Magnetic and magnetotransport properties at ambient pressure and ferro- to antiferromagnetic transition under pressure, S. Polesya, S. Mankovsky, H. Ebert, P. G. Naumov, M. A. ElGhazali, W. Schnelle, S. Medvedev, S. Mangelsen, and W. Bensch, Phys. Rev. B **102** (2020) 174423.*

[5]* *Pressure-induced collapse of large-moment magnetic order and localized-to-itinerant electronic transition in the host-guest compound $[Cs_6Cl][Fe_{24}Se_{26}]$, P. Adler , S. A. Medvedev , M. Valldor, P. G. Naumov, M. A. ElGhazali, and R. Rüffer, Phys. Rev. B **101** (2020) 094433.*

[6] *Pressure-induced superconductivity and modification of Fermi surface in type-II Weyl semimetal $NbIrTe_4$, Q. Mu, F. Fan, H. Borrmann, W. Schnelle, Y. Sun, C. Felser, and S. Medvedev, npj Quantum Materials **6** (2021) 55.*

[7] *Suppression of axionic charge density wave and onset of superconductivity in the chiral Weyl semimetal Ta_2Se_8I, Q. Mu, D. Nenno, Y. Qi, F. Fan, C. Pei, M. ElGhazali, J. Gooth, C. Felser, P. Narang, and S. Medvedev, submitted to Phys Rev. Materials (2021), arxiv: 2010.07345v1.*

[#] Sergiy.Medvediev@cpfs.mpg.de